levels in the field-collected colonies were determined using a Carlo Erba NA1500 NCS system. For *Trichodesmium* chlorophyll biomass, the contents of whole 10-l Niskin bottles from stratified depths were gravity filtered onto 5- to 10-μm polycarbonate filters and trichome density determined by direct microscopic enumeration using phycoerythrin epifluorescence. *Trichodesmium* trichome density was converted to chlorophyll terms by a factor derived from direct extraction and determination of chlorophyll per trichome and per colony at each station. *Trichodesmium* biomass was then integrated to the upper 50 m. Standard hydrographic parameters (temperature *T*, salinity *S* and density σ_t) were measured by CTD (conductivity–temperature–depth) at each sampling location.

1. Karl, D. M. *et al.* Ecosystem changes in the north Pacific subtropical gyre attributed to the 1991–92 El Niño. *Nature* **373,** 230–234 (1995).
2. Falkowski, P. G. Evolution of the nitrogen cycle and its influence on the biological sequestration of CO_2 in the ocean. *Nature* **387,** 272–275 (1997).
3. Capone, D. G., Zehr, J. P., Paerl, H. W., Bergman, B. & Carpenter, E. J. *Trichodesmium,* a globally significant marine cyanobacterium. *Science* **276,** 1221–1229 (1997).
4. Karl, D. M., Letelier, R., Tupas, L., Dore, J., Christian, J. & Hebel, D. The role of nitrogen fixation in biogeochemical cycling in the subtropical North Pacific Ocean. *Nature* **388,** 533–538 (1997).
5. Rueter, J. G., Hutchins, D. A., Smith, R. W. & Unsworth, N. L. in *Marine Pelagic Cyanobacteria: Trichodesmium and Other Diazotrophs* (eds Carpenter, E. J., Capone, D. G. & Rueter, J. G.) 289–306 (Kluwer, Norwell, 1992).
6. Raven, J. A. The iron and molybdenum use efficiencies of plant growth with different energy, carbon and nitrogen sources. *New Phytol.* **109,** 279–287 (1988).
7. Michaels, A. F. *et al.* Inputs, losses and transformations of nitrogen and phosphorus in the pelagic North Atlantic Ocean. *Biogeochemistry* **35,** 181–226 (1996).
8. Brand, L. Minimum iron requirements of marine phytoplankton and the implications for the biogeochemical control of new production. *Limnol. Oceanogr.* **36,** 1756–1771 (1991).
9. Schmidt, M. A. & Hutchins, D. A. Size-fractionated biological iron and carbon uptake along a coastal to offshore transect in the NE Pacific. *Deep Sea Res. II* **46,** 2487–2503 (1999).
10. Johnson, K. S., Chavez, F. P. & Friederich, G. E. Continental-shelf sediment as a primary source of iron for coastal phytoplankton. *Nature* **398,** 697–700 (1999).
11. Flynn, K. J. & Hipin, C. R. Interactions between iron, light, ammonium and nitrate: insights from the construction of a dynamic model of algal physiology. *J. Phycol.* **35,** 1171–1190 (1999).
12. Raven, J. A., Evans, M. C. W. & Korb, R. E. The role of trace metals in photosynthetic electron transport in O_2-evolving organisms. *Photosynth. Res.* **60,** 111–149 (1999).
13. Landing, W. M. & Bruland, K. W. The contrasting biogeochemistry of iron and manganese in the Pacific Ocean. *Geochim. Cosmochim. Acta* **51,** 29–43 (1987).
14. Duce, R. A. & Tindale, N. W. Atmospheric transport of iron and its deposition in the ocean. *Limnol. Oceanogr.* **36,** 1715–1726 (1991).
15. Rutgers van der Loeff, M., Helmers, E. & Kattner, G. Continuous transects of cadmium, copper, and aluminum in surface waters of the Atlantic ocean, 50° N to 50° S: Correspondence and contrast with nutrient-like behaviour. *Geochim. Cosmochim. Acta* **61,** 47–61 (1997).
16. Wu, J., Sunda, W., Boyle, E. A. & Karl, D. M. Phosphate depletion in the western North Atlantic Ocean. *Science* **289,** 759–762 (2000).
17. Gruber, N. & Sarmiento, J. Global patterns of marine nitrogen fixation and denitrification. *Glob. Biogeochem. Cycles* **11,** 235–266 (1997).
18. Mague, T. H., Mague, F. C. & Holm-Hansen, O. Physiology and chemical composition of nitrogen-fixing phytoplankton in the central north Pacific ocean. *Mar. Biol.* **41,** 213–227 (1977).
19. Carpenter, E. J. & Price, C. C. Marine Oscillatoria (Trichodesmium) explanation for aerobic nitrogen fixation without heterocysts. *Science* **191,** 1278–1280 (1976).
20. Carpenter, E. J. & Roenneberg, T. The marine planktonic cyanobacteria *Trichodesmium* spp.: photo-synthetic rate measurements in the SW Atlantic ocean. *Mar. Ecol. Prog. Ser.* **118,** 267–273 (1995).
21. Postgate, J. *Nitrogen Fixation* 3rd edn 1–120 (Cambridge Univ. Press, Cambridge, 1998).
22. Coale, K. H. *et al.* A massive phytoplankton bloom induced by an ecosystem-scale iron fertilization experiment in the equatorial Pacific ocean. *Nature* **383,** 495–501 (1996).
23. Zwiers, F. W. & Kharin, V. V. Changes in the extremes of the climate simulated by CCC GCM2 under CO_2 doubling. *J. Clim.* **11,** 2200–2222 (1988).
24. Lagerloef, G. S. E., Lukas, R., Weller, R. A. & Anderson, S. P. Pacific warm pool temperature regulation during TOGA COARE: upper ocean feedback. *J. Clim.* **11,** 2297–2309 (1998).
25. Bruland, K. W., Franks, R. P., Knauer, G. A. & Martin, J. H. Sampling and analytical methods for the determination of copper, cadmium, zinc and nickel at the nanogram per liter level in sea water. *Anal. Chim. Acta* **105,** 233–245 (1979).
26. Gieskes, J. M., Gamo, T. & Brumsack, H. Chemical methods for interstitial water analysis aboard Joides Resolution. Ocean Drilling Program, Technical Report No. 15 46–47 (ODP Texas A&M University, College Station, 1991).
27. Capone, D. G. in *Handbook of Methods in Aquatic Microbial Ecology* (eds Kemp, P. F., Sherr, B. F., Sherr, E. B. & Cole, J. J.) 621–631 (Lewis, Boca Raton, 1993).
28. Kara, A. B., Rochford, P. A. & Hurlburt, H. E. An optimal definition for ocean mixed layer depth. *J. Geophys. Res.* **105,** 16803–16821 (2000).
29. Sprent, J. I. & Raven, J. A. Evolution of nitrogen-fixing symbioses. *Proc. R. Soc. Edinburgh B* **85,** 215–237 (1985).
30. Zehr, J. P., Harris, D., Dominic, B. & Salerno, J. Structural analysis of the Trichodesmium nitrogenase iron protein: implications for aerobic nitrogen fixation activity. *FEMS Microbiol. Lett.* **153,** 303–309 (1997).

Preservation of ancient and fertile lithospheric mantle beneath the southwestern United States

Cin-Ty Lee*†, Qingzhu Yin*, Roberta L. Rudnick*† & Stein B. Jacobsen*

* *Department of Earth and Planetary Sciences, Harvard University, 20 Oxford Street, Cambridge, Massachusetts 02138, USA*

Stable continental regions, free from tectonic activity, are generally found only within ancient cratons—the centres of continents which formed in the Archaean era, 4.0–2.5 Gyr ago. But in the Cordilleran mountain belt of western North America some younger (middle Proterozoic) regions have remained stable[1,2], whereas some older (late Archaean) regions have been tectonically disturbed[1,3], suggesting that age alone does not determine lithospheric strength and crustal stability. Here we report rhenium–osmium isotope and mineral compositions of peridotite xenoliths from two regions of the Cordilleran mountain belt. We found that the younger, undeformed Colorado plateau is underlain by lithospheric mantle that is 'depleted' (deficient in minerals extracted by partial melting of the rock), whereas the older (Archaean), yet deformed, southern Basin and Range province is underlain by 'fertile' lithospheric mantle (not depleted by melt extraction). We suggest that the apparent relationship between composition and lithospheric strength, inferred from different degrees of crustal deformation, occurs because depleted mantle is intrinsically less dense than fertile mantle (due to iron having been lost when melt was extracted from the rock). This allows the depleted mantle to form a thicker thermal boundary layer[4] between the deep convecting mantle and the crust, thus reducing tectonic activity at the surface. The inference that not all Archaean crust developed a strong and thick thermal boundary layer leads to the possibility that such ancient crust may have been overlooked because of its intensive reworking or lost from the geological record owing to preferential recycling.

The North American Cordillera is a broad continental region marked by a long period of tectonic activity, which began in the Palaeozoic era with a series of mountain-forming events and culminated in the Cenozoic era with extension[5]. Deformation appears to be heterogeneously distributed (Fig. 1). The Basin and Range province, which includes much of Nevada and southeastern California, experienced crustal thickening and subsequent large-scale extension (possibly up to 200%)[6]. In contrast, the Colorado plateau, an elevated circular region surrounded on all sides by deformed crust, has remained an island of tectonic quiescence, as evidenced by flat-lying, unfolded and largely unfaulted Palaeozoic sedimentary strata[7].

Given the relative differences in the degree of deformation seen in the overlying crust[5] and the correlation between age and stability observed elsewhere in the continents, the more-tectonized Basin and Range lithosphere might be expected to be younger than that beneath the less-tectonized Colorado plateau. However, Sm–Nd model ages indicate that the crust in the southern Basin and Range (referred to here as Mojavia) is older, formed in Palaeoproterozoic to Archaean times (~2.0–2.6 Gyr ago)[1,2], whereas the Colorado plateau crust formed subsequently in the middle Proterozoic (1.6–2.0 Gyr ago)[1,3]. There are two possible explanations for this unexpected relationship. First, the lithospheric mantle beneath Mojavia may not be as old as the crustal model ages indicate. This might

†Present address: Division of Geological and Planetary Sciences, California Institute of Technology, 1200 E. California Boulevard, Pasadena, California 91125, USA (C.-T.L.); Department of Geology, University of Maryland, College Park, Maryland 20742, USA (R.L.R.).

 69

occur if the Nd model ages reflect mixing between juvenile middle Proterozoic crust and sedimentary material shed from an adjacent Archaean craton at the time of lithosphere formation[1], or the original ancient lithospheric mantle was removed (as recently suggested for the deep lithosphere of the Sierra Nevada[8]). Second, the lithospheric mantle beneath both regions may be the same age as the overlying crust[9], but the ancient lithospheric mantle beneath Mojavia is inherently weaker than typical cratonic lithospheric mantle owing to a more fertile composition[4,10] and/or the presence of water[11]. We evaluate these two alternatives using Os model ages of peridotite xenoliths recently derived from the lithospheric mantle in both regions.

Assuming that partial melting leads to stabilization of the lithospheric mantle, the Re–Os isotope systematics of peridotite xenoliths (samples of the lithospheric mantle) can be used to date this time of stabilization; this is because partial melting fractionates Re/Os (Re is moderately depleted and Os is sequestered in the residue[12]). As ^{187}Re decays to ^{187}Os (half life of ~42 Gyr), the residue evolves towards unradiogenic $^{187}Os/^{188}Os$ and diverges from the isotopic trajectory of undepleted convecting mantle[12]. Analogous to Sm–Nd model ages, the time at which melt extraction occurred is determined from the intersection of the two isotopic evolution paths, as constrained by the present-day $^{187}Os/^{188}Os$ and $^{187}Re/^{188}Os$ ratios of the sample and the convecting mantle. Because the Os concentration in peridotites is 10–1,000 times greater than that of silicate melts or other metasomatic agents, the Os isotope system in peridotites is considerably more robust to changes imparted by metasomatism and contamination than are isotope systems based on incompatible elements, such as Sm–Nd and Rb–Sr.

The peridotite xenoliths come from the Pliocene Cima volcanic field, located in the Mojavia province, California, and from Miocene-Oligocene minette plugs located in the 'Four corners' region of the Colorado plateau. The Cima peridotites are fresh and devoid of hydrous minerals, while the Colorado plateau samples are partly serpentenized. The Mojavian samples have $^{187}Os/^{188}Os$ ratios ranging from chondritic to relatively unradiogenic values (see Supplementary Information). The latter reflect long-term isolation in a low Re/Os environment produced by ancient partial melting. The samples show a positive correlation on an isochron plot, with a slope corresponding to an age of 2.5 ± 1.6 Gyr and an initial $^{187}Os/^{188}Os$ of ~0.112 (Fig. 2a). Using Al_2O_3 as a proxy for the Re/Os ratio[13] results in an initial $^{187}Os/^{188}Os$ of ~0.113 (Fig. 2b), indicating that depletion in Re and Al probably reflect the same ancient partial melting event. The oldest Re depletion age (assuming Re/Os = 0) for the Mojave samples is 2.4 Gyr ($^{187}Os/^{188}Os$ = 0.1120). Although this represents a minimum age, this sample's $^{187}Os/^{188}Os$ may closely approximate the 'true' initial ratio because its Al_2O_3 content (0.68 wt%) is below the lower limit (0.7 wt%) at which
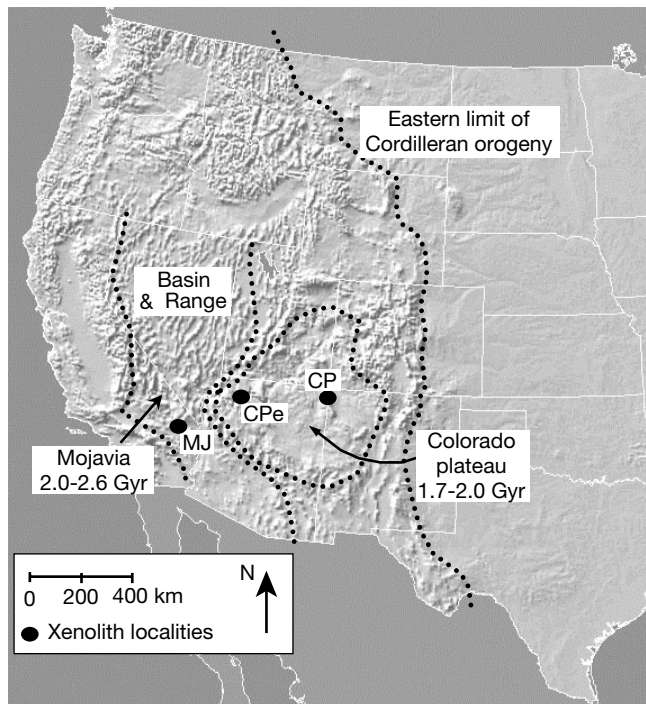

Figure 1 Digital elevation map showing topographic features within the Cordilleran orogenic belt, most of which are associated with late Cenozoic tectonism. The Colorado plateau is an elevated region of mostly undeformed sedimentary strata, surrounded on all sides by regions that have undergone compression and/or extension. Ages represent Sm–Nd crust formation ages[1,2]. Xenolith localities are indicated: CP, central Colorado plateau (The Thumb volcanic dyke); CPe, edge of Colorado plateau (Grand Canyon volcanic field); and MJ, Mojavia (Cima volcanic field).
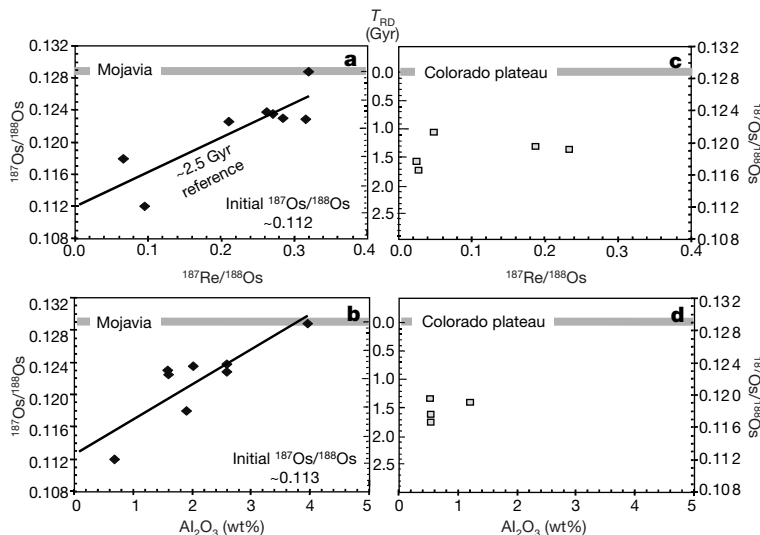

Figure 2 Re–Os isotopic constraints on the age of lithospheric mantle beneath Mojavia and the Colorado plateau. Top panels, Re–Os isotope data (**a**, Mojavia; **c**, Colorado plateau). Bottom panels, Al_2O_3 content (wt%) used as a proxy for Re/Os (**b**, Mojavia; **d**, Colorado plateau). T_{RD} represents Re-depletion model ages, calculated by assuming Re/Os = 0 and extraction from a primitive upper mantle[12] (grey horizontal bar).

Re/Os is suggested to drop to zero during partial melting of the upper mantle[14]. Re–Os model ages on individual samples range between 1.8 and 3.4 Gyr (except for Ki5-139). Collectively, these data point to a late Archaean or earliest Proterozoic age for lithospheric mantle formation beneath Mojavia. This age is consistent with the Sm–Nd model ages of the overlying crust, which thus appear to represent accurately the timing of crust formation[1,2,9].

The Colorado plateau samples (see Supplementary Information) plot along a horizontal array on a Re–Os isochron diagram (Fig. 2c), which does not give any meaningful age significance. Instead, the array is probably due to recent addition or loss of Re (ref. 12). Although the data also do not define a strong correlation between $^{187}Os/^{188}Os$ and Al_2O_3 content (Fig. 2d), the low Al_2O_3 contents and $^{187}Os/^{188}Os$ imply that most of the Re was depleted during a partial melting event, which occurred ~1.6 Gyr ago (Fig. 2c, d), within uncertainty of Sm–Nd model ages of eclogitic xenoliths from the same region[3] and consistent with evidence for old Nd in the lithospheric mantle beneath the Colorado plateau[15,16].

Our data not only confirm that ancient lithospheric mantle persists beneath the southwestern USA despite the protracted Cordilleran orogeny, but also show that the age of the lithospheric

mantle beneath each province is indistinguishable from Nd model ages of the overlying crust. Thus continental lithospheric strength is not strictly a function of the formation age of the lithospheric mantle, as might be inferred from the stability of Archaean cratons.

Instead, bulk composition may control the strength of continental lithospheric mantle, by controlling its ultimate thickness. To quantify composition, we use the Mg number (Mg# is the molar Mg/(Mg+Fe) ratio) of a peridotite as a measure of the degree of depletion. This number is an inverse measure of the amount of Fe, and the higher the Mg#, the lower the density. The mode Mg# for the lithospheric mantle of strong Archaean cratons, such as Tanzania[17,18], South Africa[19,20] and Siberia[21], is 0.93, for the weak Palaeoproterozoic to Archaean Mojavia province it is 0.90 (based on compilations in ref. 22 and our own data), and for the strong Proterozoic Colorado plateau it is 0.91 (refs 15, 23) (Fig. 3). Previous studies have shown that most Archaean cratons are underlain by more depleted mantle than post-Archaean regions, leading to an apparent correlation between strength and bulk composition. Our work corroborates these findings by showing that even when age–strength correlations break down, bulk composition still influences lithospheric strength.

Motivated by seismological evidence and the lack of a strong correlation between continents and the long-wavelength geoid, Jordan suggested that continents are underlain by thermal boundary layers, stabilized against convective disruption by compositional buoyancy[4]. This condition, known as the 'isopycnic hypothesis', requires that the negative buoyancy imposed by the colder thermal state of the mantle beneath continents is exactly compensated by a lower intrinsic density of the mantle beneath continents at every level within the viscous thermal boundary layer (but below the elastic mechanical boundary layer). Figure 4 shows isopycnic density curves calculated (see Methods) for various ocean–continent
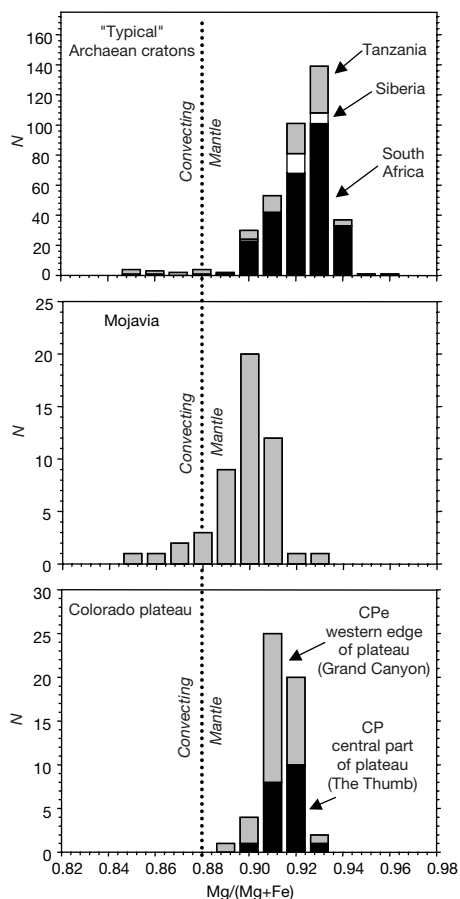

Figure 3 Comparison of the bulk Mg# of lithospheric mantle beneath typical Archaean cratons, the tectonized Mojavia block, and the strong Colorado plateau, N, number of samples. Top, a compilation of bulk-rock Mg# for low-temperature peridotites from the Tanzanian[17,18], Siberian[21] and South African cratons[19,20]. High-temperature sheared peridotites were not included in the compilation because these may have been recently refertilized by magmatic processes shortly before eruption. Middle, data from Mojavian xenolith localities based on bulk-rock compilations from ref. 22 and our own data set (olivine compositions). Bottom, data from Colorado plateau samples, which include peridotites from the western edge of the plateau (Grand Canyon[15]) and from central part of the plateau (the 'Four corners' region[10,23]). The estimated Mg# for the convecting upper mantle is taken to be ~0.88 (shown as a vertical dotted line).
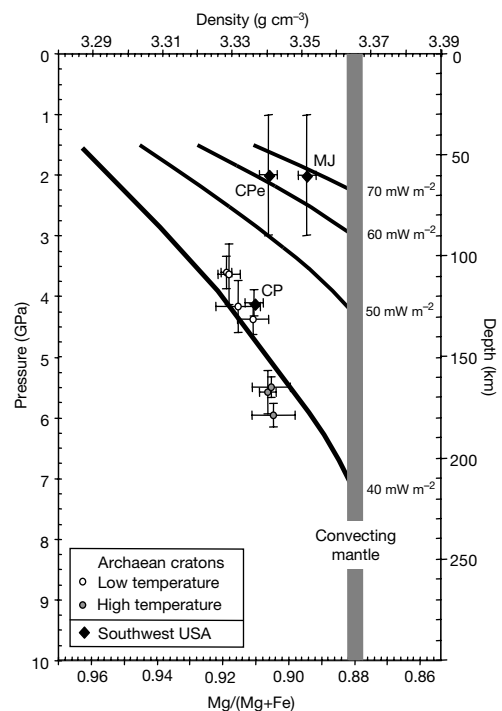

Figure 4 Isopycnic density curves, illustrating the role of bulk composition in determining lithospheric thickness. Curves were calculated for a range of surface heat flows: 70, 60, 50 and 40 mW m^{-2}. MJ, CP and CPe are defined in Fig. 1 legend. Unlabelled points refer to data from different xenolith suites from the Siberian, Tanzanian, and South African cratons (high-temperature peridotites are also shown for reference). Each symbol represents the average density and pressures of all xenoliths within a given xenolith suite. See Methods for details.

temperature differences for a range of surface heat flows and parameters given in the figure legend[24] and in Methods. Although the absolute positions of the isopycnic lines depend strongly on the assumed parameters (namely, crustal heat production and potential temperature of the convecting mantle adiabat), Fig. 4 illustrates that relative differences in bulk composition translate into differences in the thickness of the thermal boundary layer regardless of any uncertainty in the above parameters. The isopycnic hypothesis thus explains the observed correlation between strength and bulk composition because more depleted mantle generates a thicker, colder and hence stronger thermal boundary layer, whereas more-fertile mantle allows for a thinner, hotter and hence weaker thermal boundary layer.

Because the Mojavian peridotites are more fertile than typical cratonic mantle and derive from shallower depths (based on the lack of garnet), they plot on a warmer isopycnic curve ($\sim$70 mW m^{-2}), whereas the xenoliths from the centre of the Colorado plateau (garnet-bearing) plot near the array defined by peridotites from stable Archaean cratons. Ignoring localized regions of high heat flow attributed to recent magmatism, we note that the measured surface heat flow for Mojavia is 60–80 mW m^{-2} and that for the Colorado plateau ranges to lower values (40–80 mW m^{-2})[25]. If all of these regions originally fit the isopycnic condition, as is probably the case, given the lack of large negative geoid or free air gravity anomalies over continents[26], the more-fertile character of the Mojavia mantle requires a thinner thermal boundary layer (50–100 km) than that beneath the more-depleted Colorado plateau and stable Archaean cratons ($\sim$200 km). This is consistent with the lack of garnet in Mojavian xenoliths (implying lithospheric thicknesses less than $\sim$90 km) and the presence of garnet in the Colorado plateau xenoliths. Thermobarometric data on the latter (calculated from the data of ref. 23) show that the Colorado plateau lithosphere extended to at least 120 km depth at the time of xenolith sampling. In this context, we note that spinel peridotite xenoliths from the western edge of the Colorado plateau[10,15] plot along an isopycnic line intermediate between Mojavia and the central Colorado plateau, suggesting that the Colorado plateau lithospheric mantle is thickest at its centre.

The correlation between strength and bulk composition can be explained if the latter dictates the ultimate thickness to which the thermal boundary layer can grow beneath continents, in turn controlling lithospheric strength by defining the thickness of the lithosphere itself. Further thickening of the thermal boundary layer beyond that allowed by the bulk Mg# of the lithospheric mantle would result in this mantle becoming unstable due to its increased negative thermal buoyancy. We suggest that the low viscosity imposed on the residual peridotite by the high temperatures associated with the melting event may have been compensated by a viscosity increase produced by complete dehydration, thus explaining how originally hot, depleted mantle may have eventually stabilized to form thick lithospheric mantle[11,27].

Our findings also have implications for interpreting the ancient rock record. As the Earth may have been hotter and convecting more vigorously in the past, there may have been a secular decrease in the degree of melting, resulting in an apparent correlation between lithospheric mantle composition, and hence lithospheric strength, with age. However, the unusually fertile, ancient lithospheric mantle in the Mojavia province raises the question of how much Archaean lithosphere, characterized by only minor depletion, may have been lost from the geologic record by recycling back into the mantle. If this has occurred, the present distribution of Archaean crust may thus represent a biased sampling of crust underlain by highly depleted mantle (as suggested, for example, in ref. 28). Alternatively, the fact that Mojavian lithospheric mantle still persists despite its fertility may mean that even minor depletion is sufficient to inhibit recycling of continental lithosphere. However, because of its weaker character, such fertile, ancient lithosphere may be more easily overlooked and mistaken for Phanerozoic material on the basis of the degree of deformation or metamorphic age. □

Methods

Calculation of isopycnic density curves

These curves (Fig. 4) were calculated from $\Delta\rho(z) = \rho^0\alpha\Delta T(z)$, where ρ^0 is the normative density (at STP) of the fertile convecting mantle beneath oceans (grey vertical bar), α is the thermal expansion (2.7 × 10^{-5} per °C), and $\Delta T(z)$ is the continent–ocean temperature difference as a function of depth z (ref. 4). Values of $\Delta T(z)$ were determined by assuming a 1,300 °C potential adiabat for the convecting mantle (adiabatic temperature gradient of 0.5 °C km^{-1}), and continental geotherms with a range of surface heat flows; we assume that heat production of the crust and mantle is 0.5 μW m^{-3} and 0.02 μW m^{-3} (refs 24, 25), respectively. This crustal heat-production value was chosen so that the average pressures and densities of peridotite xenoliths from the stable Archaean Tanzanian, Siberian and South African cratons approximately coincide with an isopycnic curve derived for a surface heat flow of 40 mW m^{-2}, the average measured on stable Archaean cratons[29]. This choice of crustal heat production is within the range allowed by xenolith thermobarometry[24]. Densities were calculated using an empirical correlation between bulk Mg# and density (in g cm^{-3}), $\rho = 4.201 - 0.950$Mg# ($r^2 = 0.74$) from a suite of well-characterized xenoliths from Tanzania[18]. Error bars in Fig. 4 represent the $2\sigma_{mean}$ of the entire population of densities (obtained by propagating the $2\sigma_{mean}$ of Mg#s through the above equation) and pressures for a given xenolith suite (errors in the thermobarometric equation or the equation for calculating density from Mg# are not included). Tanzanian densities were calculated using a linear combination of mineral endmember compositions[30] and their modal abundances (calculated by least-squares regression of whole-rock and mineral compositions). For internal consistency, the density for convecting upper mantle[31] was calculated in the same manner. Pressures for garnet-bearing peridotites (most cratonic peridotites) were calculated using thermobarometers based on the solubility of Al in orthopyroxene coexisting with garnet[32]. For spinel peridotites (for example, MJ and CPe), the pressure was estimated to be between 1 and 3 GPa, based on limits placed on the thickness of the crust and the absence of garnet.

1. Bennett, V. C. & DePaolo, D. J. Proterozoic crustal history of the western United States as determined by neodymium isotopic mapping. *Geol. Soc. Am. Bull.* **99,** 674–685 (1987).
2. Ramo, O. T. & Calzia, J. P. Nd isotopic composition of cratonic rocks in the southern Death Valley region: evidence for a substantial Archean source component in Mojavia. *Geology* **26,** 891–894 (1998).
3. Wendlandt, E., DePaolo, D. J. & Baldridge, W. S. Nd and Sr isotope chronostratigraphy of Colorado Plateau lithosphere: implications for magmatic and tectonic underplating of the continental crust. *Earth Planet. Sci. Lett.* **116,** 23–43 (1993).
4. Jordan, T. H. Composition and development of the continental tectosphere. *Nature* **274,** 544–548 (1978).
5. Burchfiel, B. C. & Davis, G. A. Nature and controls of Cordilleran orogenesis, western United States: extensions of an earlier synthesis. *Am. J. Sci.* **275,** 363–396 (1975).
6. Wernicke, B., Axen, G. J. & Snow, J. K. Basin and Range extensional tectonics at the latitude of Las Vegas, Nevada. *Geol. Soc. Am. Bull.* **100,** 1738–1757 (1988).
7. Dickinson, W. R. in *Geologic Evolution of Arizona* (eds Jenney, J. P. & Reynolds, S. J.) 1–16 (Arizona Geological Society Digest, Vol. 17, Arizona Geological Survey, Tucson, AZ, 1989).
8. Lee, C.-T., Yin, Q.-Z., Rudnick, R. L., Chesley, J. T. & Jacobsen, S. B. Os isotopic evidence for Mesozoic removal of lithospheric mantle beneath the Sierra Nevada, California. *Science* **289,** 1912–1916 (2000).
9. Wooden, J. L. & Miller, D. M. Chronologic and isotopic framework for early Proterozoic crustal evolution in the eastern Mojave desert region, SE California. *J. Geophys. Res.* **95,** 20133–20146 (1990).
10. Smith, D. Insights into the evolution of the uppermost continental mantle from xenolith localities on and near the Colorado Plateau and regional comparisons. *J. Geophys. Res.* **105,** 16769–16781 (2000).
11. Pollack, H. N. Cratonization and thermal evolution of the mantle. *Earth Planet. Sci. Lett.* **80,** 175–182 (1986).
12. Walker, R. J., Carlson, R. W., Shirey, S. B. & Boyd, F. R. Os, Sr, Nd, and Pb isotope systematics of southern African peridotite xenoliths: implications for the chemical evolution of subcontinental mantle. *Geochim. Cosmochim. Acta* **53,** 1583–1595 (1989).
13. Reisberg, L. & Lorand, J.-P. Longevity of sub-continental mantle lithosphere from osmium isotope systematics in orogenic peridotite massifs. *Nature* **376,** 159–162 (1995).
14. Handler, M. R. & Bennett, V. C. Behaviour of platinum-group elements in the subcontinental mantle of eastern Australia during variable metasomatism and melt depletion. *Geochim. Cosmochim. Acta* **63,** 3597–3618 (1999).
15. Alibert, C. Peridotite xenoliths from western Grand Canyon and the Thumb: a probe into the subcontinental mantle of the Colorado Plateau. *J. Geophys. Res.* **99,** 21605–21620 (1994).
16. Roden, M. F., Smith, D. & Murthy, V. R. Chemical constraints on lithosphere composition and evolution beneath the Colorado Plateau. *J. Geophys. Res.* **95,** 2811–2831 (1990).
17. Rudnick, R. L., McDonough, W. F. & Orpin, A. in *Proc. Vth Int. Kimberlite Conf.* Vol. 1 (eds Meyer, H. O. A. & Leonardos, O.) 336–353 (Companhia de Pesquisa de Recursos Minerais Spec. Publ. 1, Rio de Janeiro, 1994).
18. Lee, C.-T. & Rudnick, R. L. in *Proc. VIIth Int. Kimberlite Conf.* P. H. Nixon Vol. (eds Gurney, J. J., Gurney, J. L., Pascoe, M. D. & Richardson, S. H.) 503–521 (Red Roof Design, Cape Town, 1999).
19. Boyd, F. R. & Mertzman, S. A. in *Magmatic Processes: Physicochemical Principles* (ed. Mysen, B. O.) 13–24 (Spec. Publ. Vol. 1, Geochemical Society, University Park, Pennsylvania, 1987).
20. Winterburn, P. A., Harte, B. & Gurney, J. J. Peridotite xenoliths from the Jagersfontein kimberlite pipe: I. Primary and primary-metasomatic mineralogy. *Geochim. Cosmochim. Acta* **54,** 329–341 (1990).
21. Boyd, F. R. et al. Composition of the Siberian cratonic mantle: evidence from Udachnaya peridotite xenoliths. *Contrib. Mineral. Petrol.* **128,** 228–246 (1997).

22. Wilshire, H. G., McGuire, A. V., Noller, J. S. & Turin, B. D. Petrology of lower crustal and upper mantle xenoliths from the Cima volcanic field, California. *J. Petrol.* **32**, 169–200 (1991).

23. Ehrenberg, S. N. Petrogenesis of garnet lherzolite and megacrystalline nodules from the Thumb, Navajo Volcanic field. *J. Petrol.* **23**, 507–547 (1982).

24. Rudnick, R. L., McDonough, W. F. & O'Connell, R. J. Thermal structure, thickness and composition of continental lithosphere. *Chem. Geol.* **145**, 395–411 (1998).

25. Sass, J. H. *et al.* Thermal regime of the southern Basin and Range Province: 1. Heat flow data from Arizona and the Mojave Desert of California and Nevada. *J. Geophys. Res.* **99**, 22093–22119 (1994).

26. Shapiro, S. S., Hager, B. H. & Jordan, T. H. The continental tectosphere and Earth's long-wavelength gravity field. *Lithos* **48**, 135–152 (1999).

27. Hirth, G., Evans, R. L. & Chave, A. D. Comparison of continental and oceanic mantle electrical conductivity: is the Archean lithosphere dry? *Geochem. Geophys. Geosys.* [online] 〈http://146.201.254.53/publicationsfinal/articles/2000GC000048/article2000GC000048.pdf〉 (2000).

28. Bowring, S. A. & Housh, T. The Earth's early evolution. *Science* **269**, 1535–1540 (1995).

29. Nyblade, A. A. & Pollack, H. N. A global analysis of heat flow from Precambrian terrains: implications for thermal structure of Archean and Proterozoic lithosphere. *J. Geophys. Res.* **98**, 12207–12218 (1993).

30. Bass, J. D. in *Mineral Physics and Crystallography: A Handbook of Physical Constants* (ed. Ahrens, T. J.) 45–63 (American Geophysical Union, Washington, District of Columbia, 1995).

31. McDonough, W. F. The composition of the Earth. *Chem. Geol.* **120**, 1535–1540 (1995).

32. Brey, G. P. & Kohler, T. Geothermobarometry in four-phase lherzolites II. New thermobarometers, and practical assessment of existing thermobarometers. *J. Petrol.* **31**, 1353–1378 (1990).

Consistent patterns and the idiosyncratic effects of biodiversity in marine ecosystems

Mark C. Emmerson*, Martin Solan*, Chas Emes*, David M. Paterson† & Dave Raffaelli*‡

* Culterty Field Station, University of Aberdeen, Newburgh, Ellon, AB41 6AA, Scotland

† Gatty Marine Laboratory, University of St Andrews, St Andrews, Fife, KY16 8LB, Scotland

Revealing the consequences of species extinctions for ecosystem function has been a chief research goal[1–7] and has been accompanied by enthusiastic debate[8–11]. Studies carried out predominantly in terrestrial grassland and soil ecosystems have demonstrated that as the number of species in assembled communities increases, so too do certain ecosystem processes, such as productivity, whereas others such as decomposition can remain unaffected[12]. Diversity can influence aspects of ecosystem function, but questions remain as to how generic the patterns observed are, and whether they are the product of diversity, as such, or of the functional roles and traits that characterize species in ecological systems. Here we demonstrate variable diversity effects for species representative of marine coastal systems at both global and regional scales. We provide evidence for an increase in complementary resource use as diversity increases and show strong evidence for diversity effects in naturally assembled communities at a regional scale. The variability among individual species responses is consistent with a positive but idiosyncratic pattern of ecosystem function with increased diversity.

We investigated diversity–function relations in mesocosms containing a gradient of species richness, established using intertidal invertebrates. The ecosystem function that we measured was the flux of nutrients (specifically ammonia nitrogen (NH_4-N)) to the overlying water column, a microbial process essential for primary production, which is mediated through the physical working of the sediment by invertebrates[13,14].

Replicate species pools were sampled from locations around the coastlines of northeast Scotland, southwest Sweden and central south Australia. These replicate regional species pools allow us to separate the effects of species richness from any combinatorial effects that might result from species identity. Such between-site comparisons have been made in terrestrial systems[4], and the importance of environment and site effects is well recognized[15–17].

For each site we created a species richness gradient, on the basis of previous knowledge of the local species pools. Species were not selected randomly; rather, they were common species dominating the biomass at each site, and all are known to interact directly with the sediment in which they live. These simple assemblages ranged from one to four species, dependent on locality (see Methods and Supplementary Information). At these low levels of species richness, the effects of diversity are most likely to be manifest. Additionally, species were classified into one of three functional groups so that the effects of functional diversity could also be considered (see Methods). Two treatments were employed: a primary treatment of species

Table 1 Summary of ANCOVA of NH_4-N production across sites and treatments

Source of variation	d.f.	s.s.	m.s.	*F*	*P*
Combined site analysis*					
Site	3	38.108	1.723	158.71	0.001†
Biomass	1	0.937	0.346	31.93	0.001
Site*biomass	3	0.156	0.037	3.44	0.018
Species richness	1	0.058	0.05	4.65	0.032
Error	195	2.12	0.01		
Total	211	43.82			
Individual site analysis‡					
Gullmarsfjord					
Biomass	1	0.234	0.162	50.18	0.001
Species richness	1	0.055	0.017	5.31	0.024
Function richness	1	0.109	0.014	4.49	0.037
Species identity	9	0.206	0.023	7.12	0.001
Error	77	0.248	0.003		
Total	89	0.854			
Ythan a§					
Biomass	1	0.058	0.026	5.18	0.035
Species identity	3	0.067	0.022	4.4	0.016
Error	19	0.096	0.005		
Total	25	0.233			
Ythan b§					
Biomass	1	0.301	0.098	34.09	0.001
Species identity	3	0.438	0.1463	50.92	0.001
Error	40	0.114	0.002		
Total	46	0.917			
Boston bay‖					
Biomass	1	0.828	0.486	25	0.001
Error	39	0.758	0.019		
Total	48	1.732			

d.f., degrees of freedom. s.s., sum of squares. m.s., mean squares.

* Each site was treated as a replicate for the purposes of a large combined analysis. the design treated site as a factor whereas biomass, species richness and functional group richness were treated as covariates. Functional group richness terms were non-significant and are not presented here.

† Significant inter-site differences are responsible for significant species richness terms (two and four species treatments are only present at Gullmarsfjord site, which is significantly different from Ythan and Boston bay sites).

‡ Because of the significant site terms each site was analysed separately. The structure of this analysis regarded species identity (treatment identity) as the main factor, and biomass, species richness and functional group richness as covariates for the purposes of regression analysis.

§ At the Ythan estuary sites, both species richness and functional richness were non-significant (data not shown).

‖ No significant effects were found at Boston bay for species richness, functional richness or species identity.

‡ Present address: Environment Department, University of York, Heslington, York, YO10 5DD, UK.